Rare Metal Materials and Engineering
Volume 50, Issue 2, February 2021
Available online at www.rmme.ac.cn

Science Press

Cite this article as: Rare Metal Materials and Engineering, 2021, 50(2): 0475-0482.

ARTICLE

Effect of Neodymium Addition on Plate-type V_2O_5-MoO_3/ TiO_2 Catalyst for Selective Catalytic Reduction of NO

Huang Li[1], **Zong Yuhao**[1], **Wang Hu**[1], **Chang Zhengfeng**[1,2], **Zhang Shule**[2], **Zhong Qin**[2]

[1] Datang Nanjing Environmental Protection Technology Co., Ltd, Nanjing 211111, China; [2] School of Chemical Engineering, Nanjing University of Science and Technology, Nanjing 210094, China

Abstract: A series of plate-type V_2O_5-MoO_3-Nd_2O_3/TiO_2 catalysts with different amounts of neodymium were prepared to investigate the effect of neodymium addition on selective catalytic reduction (SCR) of NO with NH_3. XRD, N_2-adsorption, XPS, H_2-TPR, Raman, NH_3-TPD, and FT-IR were used to characterize the catalysts. It is found that with suitable addition of Nd (0.25wt% and 0.5wt% Nd_2O_3) to V_2O_5-MoO_3/TiO_2 catalyst not only improves the reduction property, but also increases the $O_\alpha/(O_\alpha+O_\beta)$ ratio of the catalyst, which results in the enhancement of catalytic efficiency. However, when the content of Nd_2O_3 is excessive (0.75wt% and 1wt%), the acid sites of the catalysts decrease. Accordingly, the catalytic performance of these catalysts is relatively low. Moreover, the mechanical property of the catalyst declines when the content of Nd_2O_3 is excessive. Among the catalysts investigated, VMoNd(0.5)/Ti catalyst has the best catalytic performance, and also exhibits good SO_2 and H_2O resistance.

Key words: neodymium addition; plate-type; V_2O_5-MoO_3/TiO_2; NH_3-SCR

Nitrogen oxides (NO_x) are very harmful to the ecosystem and human health because they can contribute to the formation of photochemical smog, acid rain, ozone depletion and greenhouse effect. Selective catalytic reduction with NH_3 (NH_3-SCR) is the most effective technology for removing NO_x from coal-fired power plants and V_2O_5-TiO_2 based catalysts are the key to this technology[1-3]. In practical applications, honeycomb catalysts (V_2O_5-WO_3/TiO_2) and plate-type catalysts (V_2O_5-MoO_3/TiO_2) are widely used. Due to the suitability to the high dust and high arsenic flue gas condition in NH_3-SCR system of coal-fired power plants[4], the market share of the plate-type V_2O_5-MoO_3/TiO_2 catalyst has increased significantly in the last decade. Yet the active temperature window of plate-type V_2O_5-MoO_3/TiO_2 catalyst is narrow, it is hard to be used for lower temperature of flue gas under low-load operation of coal-fired boilers. Furthermore, the low N_2 selectivity at high temperature and relatively poor mechanical property still exist in practical applications. Therefore, further investigation is still needed to improve these performances.

Previous researches have pointed out that the selection of promoter[5-7], the property of TiO_2 carrier[8-10] and catalyst preparation methods[2,11-13] have significant effects on the catalytic performance of V_2O_5-TiO_2-based catalysts. Among them, the introduction of rare earth element metals has been recognized to be an efficient and convenient way. Chen et al[5] found that Ce can obviously enhance the activity of VWTi catalyst, because it can not only improve the reduction property of VWTi catalysts via the interaction between V and W species, but also enhance the NO_x adsorption. The study reported by Ma et al [14] has confirmed that the improved low-temperature activity of VCeWTi catalyst can be attributed to the enhanced reduction property due to the formation of V-O-Ce bond. Except for the studies about improving activity mentioned above, Marzia's group[15] found that due to the interaction of V and rare earth elements (Tb, Er, Dy, Sm, and

---

Received date: February 26, 2020
Foundation item: Transformation of Scientific and Technological Achievements of Jiangsu Province of China (BA2017095); Postdoctoral Grant Grogram of Jiangsu (2018K076C); China Postdoctoral Science Foundation (2019M651632)

Corresponding author: Zhang Shule, Ph. D., Professor, School of Chemical Engineering, Nanjing University of Science and Technology, Nanjing 210094, P. R. China, Tel: 0086-25-84315517, E-mail: shulezhang@163.com

Gd), the formed rare earth vanadates remarkably enhance the thermal stability of VTi based catalysts. However, all modifications in above studies only enhance the activity or stability of VTi catalysts. Thus, the development of a feasible way to simultaneously enhance the activity and stability seems necessary.

In recent years, using neodymium (Nd) for improving NH_3-SCR catalyst has getting increasing attention. Studies reported that Nd doping can facilitate the NH_3-SCR reaction via oxidizing NO to NO_2 due to the better reduction property[16,17]. The researches on MnO_x base catalyst confirmed that Nd modification can improve the activity and SO_2 resistance[18-20]. Feng et al[21] reported that Nd modified Cu/SAPO-34 catalyst shows superior low-temperature hydrothermal stability than Cu/SAPO-34 catalyst. Casanova et al[22] found that the introduction of Nd into V_2O_5/TiO_2-WO_3-SiO_2 catalyst leads to improvement in thermal stability by hindering transformation from TiO_2 (anatase) into TiO_2 (rutile), which enhances the performance of this catalyst in mobile applications. Inspired by these, we prepared a series of Nd modified V_2O_5-MoO_3/TiO_2 catalysts for the selective catalytic reduction of NO. These catalysts were investigated by several methods, including XRD, nitrogen adsorption, XPS, H_2-TPR, Raman, NH_3-TPD, and FT-IR. The modifying effect of Nd addition to V_2O_5-MoO_3/TiO_2 catalyst on its physicochemical characteristics and catalytic behavior in the NH_3-SCR reaction was studied.

1 Experiment

1.1 Catalyst preparation

The plate-type V_2O_5-MoO_3-Nd_2O_3/TiO_2 catalysts were produced by Datang Nanjing Environmental Protection Technology Co., Ltd. First of all, ammonium metavanadate (NH_4VO_3), neodymium nitrate hexahydrate ($Nd(NO_3)_3\cdot 6H_2O$) and ammonium molybdate ($(NH_4)_6Mo_7O_{24}\cdot 4H_2O$) were dissolved in citric acid solution. And then anatase TiO_2 powder, hydroxyethylcellulose, glass fiber and water were added into this solution in sequence. The mixture was kneaded for 4 h to form catalyst paste. Subsequently, the paste was bonded to the surface of stainless steel mesh with a thickness of 0.55 mm by a pressure roller. After drying, the catalyst samples were calcined in air flow at 550 °C for 2 h. The nominal composition of the catalyst samples was 0.8% V_2O_5 and 1.5% MoO_3. Catalysts used during this investigation were abbreviated as VMoNd(w)/Ti, where w represents the mass fraction of Nd_2O_3 in the catalyst (wt%).

1.2 Catalyst characterization

X-ray diffraction (XRD) patterns of different samples were obtained on a Philips X'Pert3 power diffractometer with a copper anode tube. An angular range 2θ from 10° to 80° was recorded using step scanning and long counting times to determine the positions of TiO_2 peaks.

Nitrogen adsorption was measured on a Micromeritics ASAP 2000 adsorption and desorption apparatus. Before measurements, the samples were degassed at a temperature of 350 °C for 15 h and a vacuum was 6.65×10^{-1} Pa.

The attrition rate of the catalysts was tested by a TABER5135 abrasion machine. The samples were cut into pieces with a size of 90 mm×90 mm. After total drying, the samples were weighted and the corresponding mass was recorded as m_1. And then the samples were placed in the abrasion machine. The tested conditions were as follows: 5 min, 60 r/min, and 1.0 kg was used. Afterwards, the samples were dried and weighted again to record the mass as m_2. The method for calculating attrition rate(ξ_p) is as follows:

$$\xi_p = \frac{m_1 - m_2}{3} \qquad (\mathrm{mg}\cdot(100\ \mathrm{r})^{-1}) \qquad (1)$$

X-ray photoelectron spectra (XPS) measurements were carried out in a PHI 5000 VersaProbe system using monochromatic Al Kα radiation (1486.6 eV). Before the measurement, the catalyst was outgassed at room temperature in a UHV chamber ($<5\times10^{-7}$ Pa). The binding energy values of the XPS signals were calibrated by the C 1s peak at 284.6 eV.

Hydrogen temperature-programmed reduction (H_2-TPR) was measured in AutoChem II 2920. Prior to H_2-TPR experiments, the catalysts were dried in flowing He stream at 300 °C for 1 h. A gas mixture composed of 5% H_2 in Ar was used as the reducing gas with a flow rate of 40 mL/min. The rate of temperature rise in the H_2-TPR experiment was 10 °C/min up to 800 °C.

The Raman spectra were recorded on a Renishaw via reflex laser Raman spectrometer with an excitation wavelength of 785 nm and a laser power of 5 mW.

Ammonia temperature-programmed desorption (NH_3-TPD) was conducted with the same apparatus used for H_2-TPR measurements. The sample (0.15 g) was preheated at 300 °C for 1 h, and then cooled down to room temperature in flowing He. At this temperature, sufficient NH_3 were injected until adsorption saturation. NH_3-TPD was carried out in a temperature range from 100 °C to 600 °C with a heating rate of 10 °C/min using He (30 mL/min) as the carrier gas.

FT-IR spectra were recorded at room temperature with a Thermo Scientific Nicolet iS10 FI-IR spectrometer in the wave number range of 4000~400 cm^{-1}.

1.3 Catalyst activity evaluation

NH_3-SCR reaction was carried out in a conventional quartz tubular reactor with catalyst samples of 0.3 g. The reaction gas with a total flow rate of 1000 ml/min was composed of 500 μl/L NH_3, 500 μl/L NO, 5% O_2 and balance N_2. All catalysts were kept on stream at each test temperature for 0.5 h. The concentrations of NO, NH_3, NO_2 and N_2O were analyzed with a flue gas analyzing apparatus (Protea AtmosFIRt). NO_x conversion (%) and N_2 selectivity were defined as follows:

$$\mathrm{NO}_x\ \text{conversion}=\frac{[\mathrm{NO}]_{\mathrm{in}}-[\mathrm{NO}]_{\mathrm{out}}-[\mathrm{NO}_2]_{\mathrm{out}}}{[\mathrm{NO}]_{\mathrm{in}}}\times 100\% \tag{2}$$

$$\mathrm{N}_2\ \text{selectivity}=\frac{[\mathrm{NO}]_{\mathrm{in}}+[\mathrm{NH}_3]_{\mathrm{in}}-[\mathrm{NO}]_{\mathrm{out}}-[\mathrm{NH}_3]_{\mathrm{out}}-2[\mathrm{N}_2\mathrm{O}]_{\mathrm{out}}}{[\mathrm{NO}]_{\mathrm{in}}+[\mathrm{NH}_3]_{\mathrm{in}}-[\mathrm{NO}]_{\mathrm{out}}-[\mathrm{NH}_3]_{\mathrm{out}}}\times 100\% \tag{3}$$

2 Results and Discussion

2.1 Characterization

The XRD patterns of different catalysts are presented in Fig.1. Obviously, all the samples show a pure characteristic pattern of anatase type of TiO_2[23]. There is no significant change in full width at half maximum (FWHM) after Nd addition, so Nd has no obvious influence on the particle size of TiO_2. In addition, no diffraction peak of V_2O_5, MoO_3 and Nd_2O_3 is observed, indicating that the vanadium, molybdenum and neodymium are well-dispersed over TiO_2 support or their size is too small to be detected by XRD.

The porous properties of catalysts were studied by N_2-adsorption experiments and the results are listed in Table 1. As can be seen from Table 1, the BET surface area and BJH pore volume decrease slightly with the increases of Nd_2O_3 concentration, whereas the average pore size increases. This behavior can be presumably due to the fact that the increased metal oxides partly block the micropore structures of the TiO_2 carrier. Fig.2 shows the N_2 adsorption-desorption isotherms of different catalysts. All the samples represent type-IV sorption curves with the H3 hysteresis loops, presenting a slit-like pores feature. No significant changes can be observed in the overlapped adsorption and desorption isotherm curves of the different catalysts. These results reveal that Nd addition cannot affect the porous properties of VMo/Ti catalyst apparently.

Apart from that, it is seen from Table 1 that the present of neodymium can also affect the attrition rate of the catalyst. It is well known that the SCR catalyst will be deactivated by the scouring and erosion of fly ashes in the flue gas during the operation period. As a result, the mechanical property of the catalyst is as important as the catalytic activity. For the commercially available plate-type catalyst, the attrition rate is a significant identification parameter of the mechanical property. In China, the attrition rate of the plate-type catalyst should be below 130 mg·(100 r)$^{-1}$ to meet the requirements of Standard GB/T 31584-2015. In practice, this data is usually controlled under 80 mg·(100 r)$^{-1}$ for the high dust flue gas condition. As summarized in Table 1, the attrition rate for VMo/Ti catalyst is 63.2 mg·(100 r)$^{-1}$. With regard to the catalysts modified by Nd, when the content of Nd_2O_3 is lower than 0.5%, the attrition rate increases slightly. It is worth noting that with the further introduction of Nd (0.75wt% and 1wt% of Nd_2O_3), the attrition rate increases considerably, demonstrating that excessive addition of Nd is harmful to the mechanical property of VMo/Ti catalyst. This result may be assigned to the alternation in the viscosity of the catalyst ingredients due to the impact of Nd precursor. Excessive content of Nd_2O_3 will weaken the interaction between the ingredient and substrate distinctively, thus wearing down the mechanical property of the catalyst.

XPS spectra of catalysts are depicted in Fig.3, and the measured results are summarized in Table 2. The V 2p XPS results of different catalysts are shown in Fig.3a. V 2p is deconvoluted to three peaks of different valance states: V^{5+}

Table 1 Textural property and attrition rate of different catalysts

Sample	BET surface area/m^2·g^{-1}	Pore volume/ cm^3·g^{-1}	Pore size/ nm	Attrition rate/ mg·(100 r)$^{-1}$
VMo/Ti	83.4	0.399	19.4	63.2
VMoNd(0.25)/Ti	82.8	0.392	19.7	63.9
VMoNd(0.5)/Ti	82.2	0.385	20.4	65.7
VMoNd(0.75)/Ti	81.6	0.381	21.0	74.3
VMoNd(1)/Ti	80.5	0.374	22.2	86.8

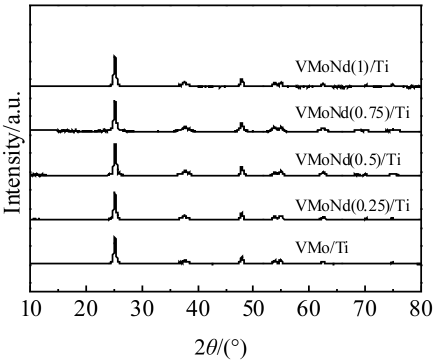

Fig.1 XRD patterns of different catalysts

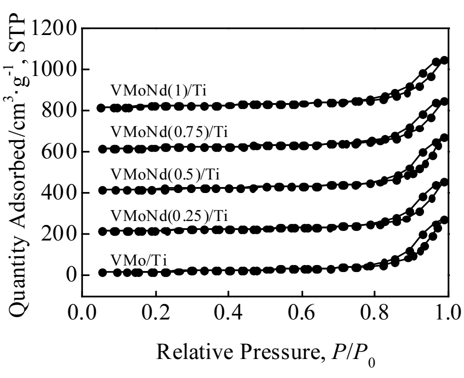

Fig.2 N_2 adsorption-desorption isotherms of different catalysts

$2p_{3/2}$ (517.2 eV), V^{4+} $2p_{3/2}$ (516.2 eV) and V^{3+} $2p_{3/2}$ (515.1 eV)[6,24]. From the data in Table 2, it is recognized that as the concentration of Nd_2O_3 increases, the values of V^{4+}/V^{5+} and $(V^{4+}+V^{3+})/V^{5+}$ ratios decrease. VMo/Ti catalyst possesses the highest value of V^{4+}/V^{5+} and $(V^{4+}+V^{3+})/V^{5+}$ ratios, meaning that a large part of vanadium exists in low oxidation states. As reported previously, the valence state of the vanadium is relevant to the structure of the vanadium oxides. Vanadium species from monomeric vanadyl exist in high oxidation states, whereas the polymeric phase corresponds to low oxidation state[25,26]. Thus, it can be deduced that the Nd addition can influence the structure of vanadium species.

Fig.3b represents the Mo 3d peak of different catalysts. The peaks at 235.4 and 232.2 eV correspond to Mo^{6+}, while the peaks at 234.7 and 231.5 eV represent Mo^{5+} [27]. For all samples, the molybdenum predominates in Mo^{6+} valence states. Furthermore, a positive relationship between $Mo^{6+}/(Mo^{5+}+Mo^{6+})$ ratio and $(V^{4+}+V^{3+})/V^{5+}$ ratio can be observed. Nonetheless, the $Mo^{6+}/(Mo^{5+}+Mo^{6+})$ ratio decreases by a small margin with decreasing the $(V^{4+}+V^{3+})/V^{5+}$ ratio. That is to say, in our experiments, the molybdenum species are not appreciably affected by Nd.

Fig.3c exhibits two peaks of O 1s, attributed to the chemisorbed oxygen (denoted as O_α) at 532.2 eV and the lattice oxygen (denoted as O_β) at 529 eV[28]. Typically, it is turned out that O_α is the most active oxygen and plays an important role in oxidation reactions[29,30]. The relatively higher $O_\alpha/(O_\alpha+O_\beta)$ ratio makes it easier to oxide NO to NO_2, which facilitates the SCR process. As listed in Table 2, the corresponding $O_\alpha/(O_\alpha+O_\beta)$ ratio for VMo/Ti catalyst is 0.16, which is lower than that of VMoNd(0.25)/Ti catalyst. Furthermore, as the amount of Nd_2O_3 increases continuously, the value of $O_\alpha/(O_\alpha+O_\beta)$ ratio increases simultaneously.

Fig.4 shows the H_2-TPR profiles of different catalysts. In view of the VMo/Ti catalyst, single reduction peak appears at 431 °C, attesting to the reduction of vanadium oxides and molybdenum species[31,32]. As the doping amount of Nd_2O_3 is 0.25wt%, it can be noted that the reduction peak area of vanadium oxides and molybdenum species increases and the peak temperature shifts slightly towards the lower region. Moreover, these change tendencies become more distinct when the amount of Nd_2O_3 is in the range of 0.5wt% to 1wt%. This result illustrates that Nd promotes the reduction property of the VMo/Ti catalyst, which is favorable to the redox reaction in the NH_3-SCR process[33]. Beyond this, additional reduction peaks can be observed at about 550 °C for VMoNd(0.75)/Ti and VMoNd(1)/Ti catalysts, which are linked with the reduction of surface neodymium oxides[19].

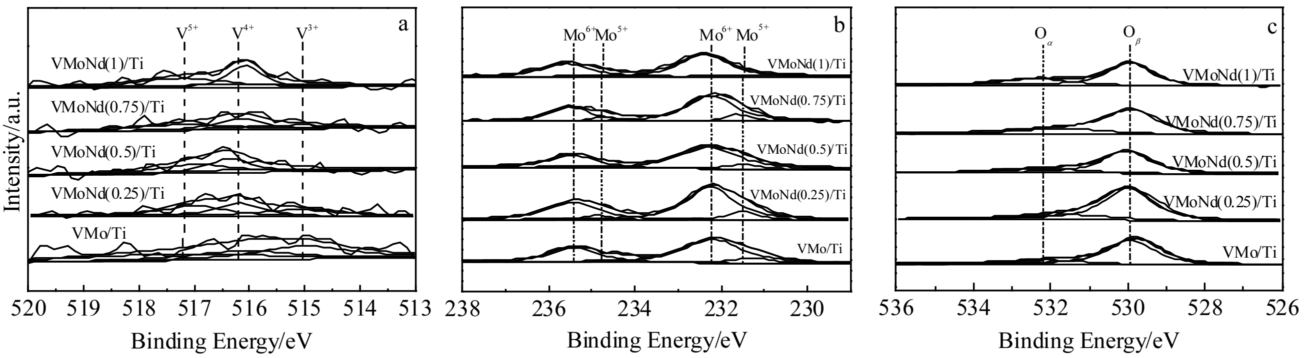

Fig.3 XPS spectra of V 2p (a), Mo 3d (b) and O 1s (c) of different catalysts

Table 2 Valence state of elements and atomic ratio for different catalysts

Catalyst	V^{4+}/V^{5+}	$(V^{4+}+V^{3+})/V^{5+}$	$Mo^{6+}/(Mo^{5+}+Mo^{6+})$	$O_\alpha/(O_\alpha+O_\beta)$
VMo/Ti	1.00	1.91	0.88	0.16
VMoNd(0.25)/Ti	0.97	1.88	0.87	0.21
VMoNd(0.5)/Ti	0.93	1.84	0.86	0.24
VMoNd(0.75)/Ti	0.91	1.78	0.86	0.26
VMoNd(1)/Ti	0.88	1.72	0.85	0.29

In general, the alteration in the reduction property of the V_2O_5-TiO_2-based catalysts may associate with the structure of the vanadium oxides. According to the previous reports[34,35], there are three main types of vanadium oxides on the surface

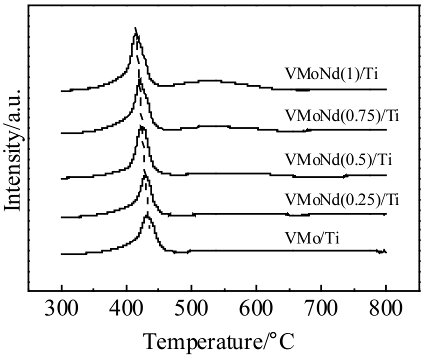

Fig.4 H_2-TPR profiles of different catalysts of TiO_2: isolated monomeric vanadyl, polymeric vanadates, and crystalline V_2O_5. The monomeric vanadyl and polymeric vanadates are referred to as "monolayer vanadia". In this experiment, the calculated V loading of different catalysts are around 1 μmol/m^2, much lower than the established value for complete monolayer (15.9 μmol/m^2)[36,37]. As a result, the vanadium oxides on the surface of TiO_2 of different catalysts exist in monolayer vanadia form. Furthermore, the isolated monomeric vanadyl is easier to be reduced than the polymeric vanadate [12]. With this line of thinking, it is reasonable to speculate that the neodymium oxides may have a "geometric effect" on the dispersion of vanadium oxides. In this circumstance, the aggregation of the vanadium oxides of the VMoNd/Ti catalysts is suppressed, which in consequence decreases the V^{4+}/V^{5+} and $(V^{4+}+V^{3+})/V^{5+}$ ratios (Fig.3) and improves the reduction property of the catalysts (Fig.4). Similar viewpoints were reported by Feng[21] and Zhang et al[38], and they found that Nd can inhibit the agglomeration of the active component over CuNd/SAPO-34 catalyst for NH_3-SCR and NiB/Bentonite catalyst for benzene hydrogenation.

In order to verify the above-mentioned inference, Raman spectroscopy were used. As presented in Fig.5, all five catalysts present three peaks around 1005, 950, and 790 cm^{-1}. The first one around 1005 cm^{-1} is assigined to the monolayer dispersion of V=O vibration from isolated monomeric vanadyl[31]. The second one at approximately 950 cm^{-1} is attributed to the V-O-V bonds from polymeric vanadate[2]. The peak at 790 cm^{-1} ascribes to crystalline Mo-O-Mo[39,40]. From Fig.5, it can be clearly seen that the Raman peak for the polymeric vanadate moves towards the lower wavenumber upon a continuous addition of Nd species. This fact allows us to confirm that the neodymium oxides affects the vanadium species. The dispersion of vanadium species is enchanced under the influence of Nd. Additionally, the peaks at 790 cm^{-1} have no obvious change, revealing that the catalysts might have a small difference in the structure of Mo species.

The surface acidity also plays a primary role in catalytic performance of V_2O_5-TiO_2-based catalysts. The acidity of the different catalysts is examined by NH_3-TPD, and the profiles are shown in Fig.6. It is clear that pure TiO_2 carrier exhibits a NH_3 desorption peak at 500 °C. When incorporated with 1wt% of Nd_2O_3, the NH_3 desorption peak disappears, suggesting that the neodymium oxides neutralize the acid sites of TiO_2. Likewise, neodymium oxides seldom provide acid sites. VMo/Ti catalyst presents a broad desorption peak with a maximum at 450 °C. In contrast, as depicted in Fig.6, a distinct decrease of ammonia desorption is observed after the loading of 0.25wt% Nd_2O_3. Meantime, the further addition of Nd leads to a monotonically decrease in ammonia adsorption. The ammonia desorption for VMo/Ti, VMoNd(0.25)/Ti, VMoNd(0.5)/Ti, VMoNd(0.75)/Ti and VMoNd(1)/Ti catalysts are 201, 125, 115, 98 and 81 μmol/g, respectively. This phenomenon elucidates that the presence of Nd decreases the amount of the acid sites of the catalysts. Additionally, it is interesting to note that the strength of acid sites in the VMoNd/Ti catalysts is weaker than that in the VMo/Ti catalyst, judging from the lower ammonia desorption temperatures.

2.2 Catalytic performance

The effect of Nd addition on the catalytic behavior of the catalysts is presented in Fig.7. From Fig.7, the VMo/Ti sample shows a relative low NO_x conversion below 340 °C. As Nd_2O_3-loading increases from 0.25wt% to 0.5wt%, a significant enhancement in the NO_x conversion at low temperatures (250~340 °C) is observed. At 280 °C, the NO_x conversion of VMo/Ti, VMoNd(0.25)/Ti and VMoNd(0.5)/Ti catalysts is 39.9%, 48.5% and 73.2%, respectively. In addition, it can be noticed also from Fig.7 that the NO_x conversion begins to decrease when the Nd_2O_3 concentration exceeds 0.5%. For the case of VMoNd(1)/Ti catalyst, the poorest catalytic activity is found. To explain these, it should be emphasized that the SCR reaction cycle encompasses four steps: (1) NH_3 is adsorbed on the Bronsted acid sites of the catalyst to form -NH^{4+}; (2) -NH^{4+} is oxidized by adjacent V^{5+}=O to form -NH_3^+ while V^{5+}=O is reduced to H-O-V^{4+}; (3) -NH^{3+} reacts with NO to form N_2 and H_2O; (4) H-O-V^{4+} is

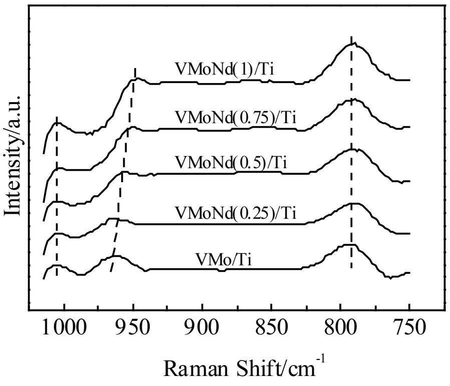

Fig.5 Raman spectra of different catalysts

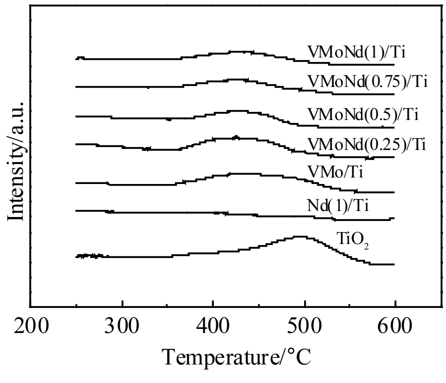

Fig.6 NH_3-TPD profiles of different catalysts oxidized to V^{5+}=O by O_2 [41,42]. The reduction property and the acidity may work collaboratively, which is significant for directing the catalytic performance. As aforementioned, the reduction properties of the VMoNd/Ti catalysts are improved by the addition of Nd. Furthermore, the $O_\alpha/(O_\alpha+O_\beta)$ ratio on catalysts surface from XPS measurement also increases continuously along with the increase of Nd content in the catalyst. As a consequence, the VMoNd(0.25)/Ti and VMoNd(0.5)/Ti catalysts display higher catalytic activity than the VMo/Ti catalyst. Concerning the samples with high Nd_2O_3 loading (>0.5wt%), although the better reduction property and higher $O_\alpha/(O_\alpha+O_\beta)$ ratio are found, the apparent decrease in the acid sites may destroy the balance between the reduction property and the acidity of the catalyst. Consequently, the catalytic performance of VMoNd(0.75)/Ti and VMoNd(1)/Ti catalysts decreases.

Fig.8 exhibits the corresponding N_2 selectivity of different catalysts. It is clear that the N_2 selectivity start to decline when the reaction temperature is higher than 340 °C, which is assigned to the fact that high reaction temperature (>350 °C) leads to the formation of N_2O[43]. Meanwhile, it is interesting to note that the addition of Nd results in the increase of the N_2 selectivity, which reaches a maximum when the content of Nd_2O_3 is 1wt%. This finding is correlated with the XPS and H_2-TPR analyses, because the polymerization process of dispersed vanadium species is usually considered as the main causes for the increase of N_2O in SCR reaction[10,44]. The loading of Nd inhibits the agglomeration of the vanadium oxides. Thereupon, the N_2 selectivity of VMoNd/Ti catalysts is enhanced.

Moreover, the resistance of VMoNd(0.5)/Ti catalyst to SO_2 and H_2O in the NH_3-SCR reaction was also studied. As shown in Fig.9, the NO_x conversion of VMoNd(0.5)/Ti catalyst at 280 °C keeps stable (about 72%) in the first 2 h. And then this data declines to 64% with the addition of 200 μl/L SO_2 and 3% H_2O. After removing SO_2 and H_2O, the NO_x conversion recovers to about 73% gradually. This result indicates that few ammonium bisulfates generate during the NH_3-SCR reaction at low temperature, which may be relevant to the low V_2O_5 content. When the reaction temperature increases to 310 °C, and 200 μl/L SO_2 and 3% H_2O are injected into the feed gases at the same time, the NO_x conversion increases to about 79%. Furthermore, when the reaction temperature up to 370 °C, the NO_x conversion increases to about 91% and then maintains this value for the next 8 h. After shutting off SO_2 and H_2O, the NO_x conversion recovers to 98% immediately.

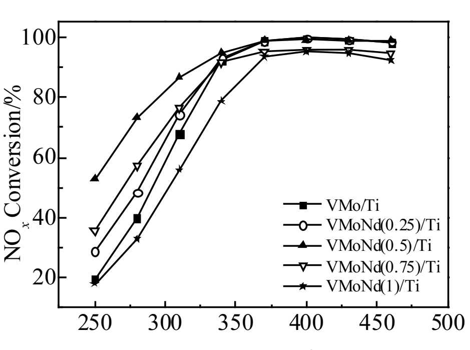

Fig.7 NO_x conversion of different catalysts

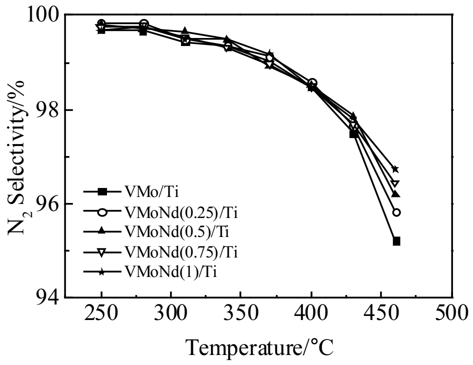

Fig.8 N_2 selectivity of different catalysts

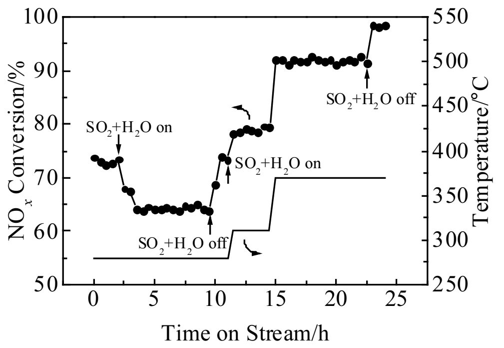

Fig.9 Effects of SO_2 and H_2O on NO_x conversion for VMoNd(0.5)/Ti catalysts

The XRD patterns and FT-IR spectra of the fresh and used VMoNd(0.5)/Ti catalysts are shown in Fig.10 and Fig.11, respectively. There is no variety in the XRD patterns of different catalysts, demonstrating that the structure of TiO_2 carrier maintains stable during the NH_3-SCR reaction process. Likewise, the FT-IR spectra of the used VMoNd(0.5)/Ti catalyst is similar to that of the fresh one. No extra adsorption bands can be observed in the FT-IR spectrum of the used VMoNd(0.5)/Ti catalyst. This result may imply that no sulfate generates after 24 h of reaction.

As a consequence of the above, the proper amount of Nd can increase the NO_x conversion, broaden the active temperature window, and enhance the N_2 selectivity of the VMo/Ti catalyst. VMoNd(0.5)/Ti catalyst not only exhibits a well catalytic activity, but also possesses good SO_2 and H_2O resistance, suggesting that VMoNd(0.5)/Ti catalyst is more

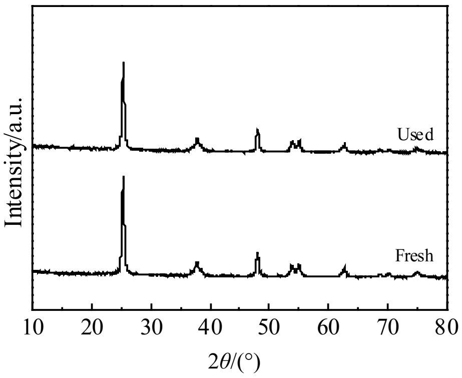

Fig.10 XRD patterns of fresh and used VMoNd(0.5)/Ti catalysts

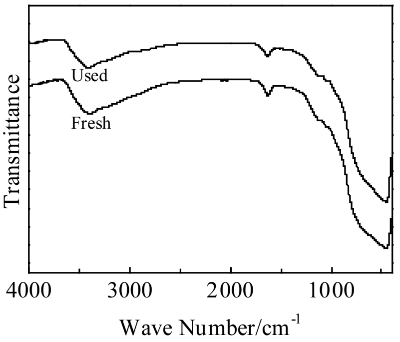

Fig.11 FT-IR spectra of fresh and used VMoNd(0.5)/Ti catalysts

excellent than the VMo/Ti catalyst for NH_3-SCR reaction.

3 Conclusions

1) Compared with the catalyst without Nd, the reduction property of VMoNd/Ti catalysts is improved. Moreover, the $O_\alpha/(O_\alpha+O_\beta)$ ratio of the catalysts also increases with the increase of Nd_2O_3 content.

2) The catalytic activity of VMoNd(0.25)/Ti and VMoNd(0.5)/Ti catalysts below 370 °C is effectively improved.

3) When the content of Nd_2O_3 in VMoNd/Ti catalyst is high (0.75wt% and 1wt%), the matching between the reduction property and the acidity of the catalyst decreases. Accordingly, the catalytic performance of these catalysts is relatively low.

4) Excess Nd has a negative effect on the mechanical property of the catalyst. In this experiments, VMoNd(0.5)/Ti catalyst exhibits the best catalytic behavior, and good SO_2 and H_2O resistance.

References

1 Liu Y M, Shu H, Xu Q S *et al. Journal of Fuel Chemistry and Technology*[J], 2015, 43(8): 1018

2 Shen Y S, Yu Y, Qiu T *et al. Rare Metal Materials and Engineering*[J], 2011, 40(6): 967 (in Chinese)

3 Kwon D W, Park K H, Hong S C. *Chemical Engineering Journal*[J], 2016, 284: 315

4 Beretta A, Lanza A, Lietti L *et al. Chemical Engineering Journal*[J], 2019, 359: 88

5 Chen L, Li J H, Ge M F. *The Journal of Physical Chemistry C*[J], 2009, 113(50): 21 177

6 Shi A J, Wang X Q, Yu T *et al. Applied Catalysis B: Environmental*[J], 2011, 106(3-4): 359

7 Zhang Q M, Song C L, Lv G *et al. Journal of Industrial and Engineering Chemistry*[J], 2015, 24: 79

8 Zhang Y P, Guo W Q, Wang L F *et al. Chinese Journal of Catalysis*[J], 2015, 36(10): 1701

9 Pan Y X, Zhao W, Zhong Q *et al. Journal of Environmental Sciences*[J], 2013, 25(8): 1703

10 Song I, Youn S H, Lee H H *et al. Applied Catalysis B: Environmental*[J], 2017, 210: 421

11 Cha W J, Chin S M, Park E *et al. Applied Catalysis B: Environmental*[J], 2013, 140-141: 708

12 Dong G J, Zhang Y F, Zhao Y *et al. Journal of Fuel Chemistry and Technology*[J], 2014, 42(12): 1455

13 Liu B, Du J, Lv X W *et al. Catalysis Science & Technology*[J], 2015, 5(2): 1241

14 Ma Z R, Wu X D, Feng Y *et al. Progress in Natural Science: Material International*[J], 2015, 25(4): 342

15 Casanova M, Schermanz K, Llorca J *et al. Catalysis Today*[J], 2012, 184(1): 227

16 Chen Y, Wang J P, Yan Z *et al. Catalysis Science & Technology*[J], 2015, 5(4): 2251

17 Jin Q J, Shen Y S, Zhu S M *et al. Journal of Materials Research*[J], 2017, 32(12): 2438

18 Chen H F, Xia Y, Fang R Y *et al. New Journal of Chemistry*[J], 2018, 42(15): 12 845

19 Guo R T, Sun P, Pan W G *et al. Industrial & Engineering Chemistry Research*[J], 2017, 56(44): 12 566

20 Huang J, Huang H, Jiang H T *et al. Catalysis Today*[J], 2019, 332: 49

21 Feng X, Lin Q J, Cao Y *et al. Journal of the Taiwan Institute of Chemical Engineers*[J], 2017, 80: 805

22 Casanova M, Rocchini E, Trovarelli A *et al. Journal of Alloys and Compounds*[J], 2006, 408-412: 1108

23 Bellifa A, Lahcene D, Tchenar YN *et al. Applied Catalysis A: General*[J], 2006, 305(1): 1

24 Guo X Y, Calvin B, William H *et al. Applied Catalysis B: Environmental*[J], 2009, 92(1-2): 30

25 Magg N, Immaraporn B, Giorgi J B *et al. Journal of Catalysis*[J], 2004, 226(1): 88

26 Broclawik E, Góra A, Najbar M. *Journal of Molecular Catalysis A: Chemical*[J], 2001, 166(1): 31

27 Al-Kandari H, Al-Kharafi F, Al-Awadi N *et al. Applied Catalysis A: General*[J], 2005, 295(1): 1

28 Kang M, Park E D, Kim J M *et al. Applied Catalysis A: General* [J], 2007, 327(2): 261

29 Jing L Q, Xu Z L, Sun X J *et al. Applied Surface Science*[J],

2001, 180(3-4): 308

30 Lin S D, Gluhoi A G, Nieuwenhuys B E. *Catalysis Today*[J], 2004, 90(1-2): 3

31 Dong G J, Bai Y, Zhang Y F *et al*. *New Journal of Chemistry*[J], 2015, 39(5): 3588

32 Casagrande L, Lietti L, Nova I *et al*. *Applied Catalysis B: Environmental*[J], 1999, 22(1): 63

33 Hu G, Yang J, Tian Y M *et al*. *Materials Research Bulletin*[J], 2018, 104: 112

34 Bulushev D A, Kiwi-Minsker L, Rainone F *et al*. *Journal of Catalysis*[J], 2002, 205(1): 115

35 Kwon D W, Park K H, Hong S C. *Applied Catalysis A: General*[J], 2013, 451: 227

36 Mutin P H, Popa A F, Vioux A *et al*. *Applied Catalysis B: Environmental*[J], 2006, 69(1-2): 49

37 Bond G C, Tahir S F. *Applied Catalysis*[J], 1991, 71(1): 1

38 Zhang R B, Li F Y, Zhang N *et al*. *Applied Catalysis A: General*[J], 2003, 239(1-2): 17

39 Mestl G. *Journal of Raman Spectroscopy*[J], 2002, 33(5): 333

40 Qiu Y, Bo L, Du J *et al*. *Chemical Engineering Journal*[J], 2016, 294: 264

41 Topsøe N Y, Topsøe H, Dumesic J A. *Journal of Catalysis*[J], 1995, 151(1): 226

42 Topsøe N Y, Dumesic J A, Topsøe H. *Journal of Catalysis*[J], 1995, 151(1): 241

43 Madia G, Elsener M, Koebel M *et al*. *Applied Catalysis B: Environmental*[J], 2002, 39(2): 181

44 Martín J A, Yates M, Ávila P *et al*. *Applied Catalysis B: Environmental*[J], 2007, 70(1-4): 330

钕的添加对 V_2O_5-MoO_3/TiO_2 平板式脱硝催化剂性能的影响

黄　力[1]，纵宇浩[1]，王　虎[1]，常峥峰[1,2]，张舒乐[2]，钟　秦[2]

(1. 大唐南京环保科技有限责任公司，江苏 南京 211111)

(2. 南京理工大学 化工学院，江苏 南京 210094)

摘　要：本研究制备了一系列不同 Nd 含量的 V_2O_5-MoO_3-Nd_2O_3/TiO_2 平板式脱硝催化剂。采用 XRD、N_2-吸附脱附、XPS、H_2-TPR、拉曼光谱、NH_3-TPD 和红外光谱等表征手段对催化剂进行分析。结果表明：适量的 Nd_2O_3(0.25%、0.5%，质量分数)可以增强 V_2O_5-MoO_3/TiO_2 催化剂的还原性能，增加了催化剂的 $O_\alpha/(O_\alpha+O_\beta)$比率，从而提升了催化剂的脱硝活性。然而，过量 Nd_2O_3 (0.75%、1%)的添加，会导致催化剂酸性性能的显著降低，造成催化剂脱硝性能的下降。此外，过量 Nd 的添加还会对催化剂的耐磨性能有负面影响。各催化剂中，VMoNd(0.5%)/Ti 催化剂显示了最佳的脱硝活性。并且，该催化剂还显示了优良的抗 SO_2、H_2O 性能。

关键词：钕添加；平板式；V_2O_5-MoO_3/TiO_2；NH_3-SCR

作者简介：黄　力，男，1986 年生，硕士，高级工程师，大唐南京环保科技有限责任公司，江苏 南京 211111，电话：025-52837798，E-mail: huangl@dteg.com.cn